Low-Energy Magnetic Excitations of the Mn_{12}-Acetate Spin Cluster Observed by Neutron Scattering

I. Mirebeau,[1] M. Hennion,[1] H. Casalta,[2] H. Andres,[3] H. U. Güdel,[3] A. V. Irodova,[4] and A. Caneschi[5]
[1]*Laboratoire Léon Brillouin, CEA-CNRS, CE Saclay, 91191 Gif-sur-Yvette, France*
[2]*Institut Laue Langevin, BP 156, F-38042 Grenoble, France*
[3]*Department of Chemistry, University of Bern, 3000 Bern 9, Switzerland*
[4]*Russian Research Center, Kurchatov Institute 123182 Moscow, Russian Federation*
[5]*Department of Chemistry, University of Florence, Via Maragliano 7, 50144, Firenze, Italy*
(Received 2 March 1999)

We studied Mn_{12}-acetate by inelastic neutron scattering and diffraction. We separated the energy levels corresponding to the splitting of the lowest S multiplet ($S = 10$ ground state). The irregular spacing of the transition energies unambiguously shows the presence of high-order terms in the spin Hamiltonian [$D = -0.457(2)$ cm^{-1}, $B_4^0 = -2.33(4) \times 10^{-5}$ cm^{-1}]. The relative intensity of the lowest energy peaks is very sensitive to the small transverse term that is responsible for quantum tunneling, providing the first determination of this term in zero magnetic field [$B_4^4 = \pm 3.0(5) \times 10^{-5}$ cm^{-1}].

PACS numbers: 75.25.+z, 75.45.+j, 78.70.Nx

Among molecular nanomagnets, the most attractive clusters consist of a few (typically 10–20) paramagnetic ions coupled by exchange interactions at the borderline between quantum and classical behavior. Besides their great theoretical interest, the study of these magnetic molecules could help to determine the size limit for information storage. Mn_{12}-acetate (Mn_{12}-ac) is the best studied spin cluster so far. In a simple ionic picture, an external ring of eight Mn III ions ($S_2 = 2$) surrounds a tetrahedron of four Mn IV ions ($S_1 = 3/2$), giving the molecule a platelike shape with tetragonal symmetry [1]. Above 10 K, a reversal of the molecular magnetization occurs by thermally overcoming the energy barrier due to uniaxial anisotropy (superparamagnetic behavior) [2]. Below 2 K, this reversal is governed by macroscopic quantum tunneling (MQT) mechanism as shown by a finite relaxation time in the magnetization at $T = 0$ [3]. Mn_{12}-ac also exhibits, as a spectacular effect, regular steps in the hysteresis cycle [4]. The thermally assisted tunneling process, which occurs within the molecular ground state, is governed by extremely small high-order spin interactions [5–7]. Mn_{12}-ac is usually described as a single spin with $S = 10$ ground state, split by anisotropy terms into sublevels with ($-10 \leq M \leq 10$). This picture assumes that the anisotropy energy is much smaller than the exchange energy. The $S = 10$ ground state corresponds to a ferrimagnetic spin arrangement of the two types of Mn ions [2,8]. On this basis, high-field–high-frequency EPR measurements were analyzed by considering spin Hamiltonian parameters up to fourth order [9]. This gave the first experimental evidence of the transverse term which was searched for in order to explain the MQT. However, depending on the range of frequency or applied field considered, different sets of parameters were reported [9,10]. Very recently, the position of the first three excited sublevels of the $S = 10$ ground state was determined by optical spectroscopy in the far infrared (IR) range [11].

In this paper, we present a detailed study of the energy sublevels of the ground state by inelastic neutron scattering (INS). Neutron scattering is the most powerful tool used to investigate spin structure and spin excitations. In contrast to EPR, it is a zero-field experiment, which requires no assumption about the Landé factor g. The INS has been used to measure exchange and anisotropy splittings in numerous clusters [12] and very recently to determine the zero-field splitting in a Fe_8 cluster [13]. In Mn_{12}-ac, we previously studied spin excitations up to 12 meV [14]. We observed several excitations attributed either to the anisotropy or to the exchange terms, and determined their dynamical form factor. The position of the anisotropy level at low temperature (1.24 meV) agreed with the EPR determination, but we were not able to resolve the detailed structure of the other sublevels at higher temperature.

Here we present results obtained with a very high energy resolution, which enable us to separate the sublevels of the ground state. The irregular spacing of the transition energies unambiguously shows the presence of high-order terms in the spin Hamiltonian. We determine these parameters up to fourth order within the single $S = 10$ ground state model. Interestingly, the intensities of the lowest energy excitations, associated with levels near the top of the barrier, are very sensitive to the value of the transverse fourth-order term, allowing the first determination of this very small term without any field perturbation.

A $[Mn_{12}O_{12}(CD_3COO)_{16}(D_2O)_4] \cdot 2CD_3COOD \cdot 4D_2O$ powder sample was synthesized using deuterated solvents, since hydrogen has a large incoherent cross section which is the main background in neutron experiments. A deuteration of 93% was achieved, as shown by the analysis of the neutron diffraction data. The crystal structure was tested

 0031-9007/99/83(3)/628(4)$15.00

between 10 and 290 K on the neutron diffractometer G6.1 at the Laboratoire Léon Brillouin. Data were analyzed with the FULLPROF program [15]. The structure keeps the tetragonal symmetry in the whole temperature range. Above 130 K the framework of the molecule, consisting of Mn, C, and O atoms, practically coincides with that determined by single crystal x-ray diffraction [1]. Only slight displacements of the acetic acid and water molecules of solvation were found. We precisely stated the positions of the H/D atoms, using common constraints for interatomic distances H-O and H-C, and angles H-O-H and H-C-H. Moreover, we determined the unknown H positions in the acetic acid molecules of solvation. Only the water molecules contain hydrogen (about 33.5%), whereas the rest of the cluster is fully deuterated. Below 130 K, we found a slight distortion of the cluster framework caused by displacements of the bridging acetate ligands. This reduces the local symmetry of Mn III with respect to room temperature, the environment of Mn IV being preserved (besides the usual lattice contraction).

The INS measurements were performed with the high-energy resolution time-of-flight spectrometer IN5 at ILL, in the temperature range 1.5–35 K. The incident wavelength was 5.9 Å, and the resolution at zero-energy transfer HWHM was 27.5 μeV. In the energy range studied $(-1.5, 1.5)$ meV, we checked that the $\mathbf{Q}$ dependence of the neutron cross section is the same for all of the inelastic transitions. It varies very little with temperature and agrees with the previous determination on a triple axis spectrometer [14]. We therefore added the contributions of all detectors, which strongly increased the statistical accuracy.

Typical spectra are shown in Fig. 1. At 1.5 K, a well-defined excitation is observed at 1.24 meV on the sample energy gain side ($\hbar\omega > 0$), with a peak width limited by the experimental resolution. It is readily attributed to an excitation from the lowest energy level ($M = \pm 10$) to the first excited level ($M = \pm 9$). The peak at 0.9 meV was already studied in [14], and its strong variation below 2.5 K suggested a close connection with the MQT. It likely arises from a fast relaxing isomer of the main Mn_{12}-ac species [16], recently used as a probe to study the dynamics in the bulk material [17]. Here this isomer is present in a very small amount(1%–2%), and its signal is neglected. The spurious temperature independent signal at the foot of the elastic peak was fitted by a Gaussian and subtracted. As the temperature increases, higher energy levels are populated, so that new excitations appear on both sides of the spectrum. At 23.8 K, we distinctly observe 14 well-separated peaks, together with much smaller ones at about ± 0.2 meV (see the inset of Fig. 1). The position of the well-resolved peaks is temperature independent. Their width, close to the resolution limit, increases with temperature of about 25% between 1.5 and 25 K, suggesting a finite lifetime. The energy intervals between adjacent peaks in the spectrum show a small but significant decrease with decreasing energy transfer. Below 25 K, the temperature evolution of the peak intensities reflects the depopulation of the lowest level at the benefit of the excited levels within the ground state manifold. Above 25 K, all peaks broaden and the total inelastic intensity decreases, as the levels attributed to higher spin states become populated.

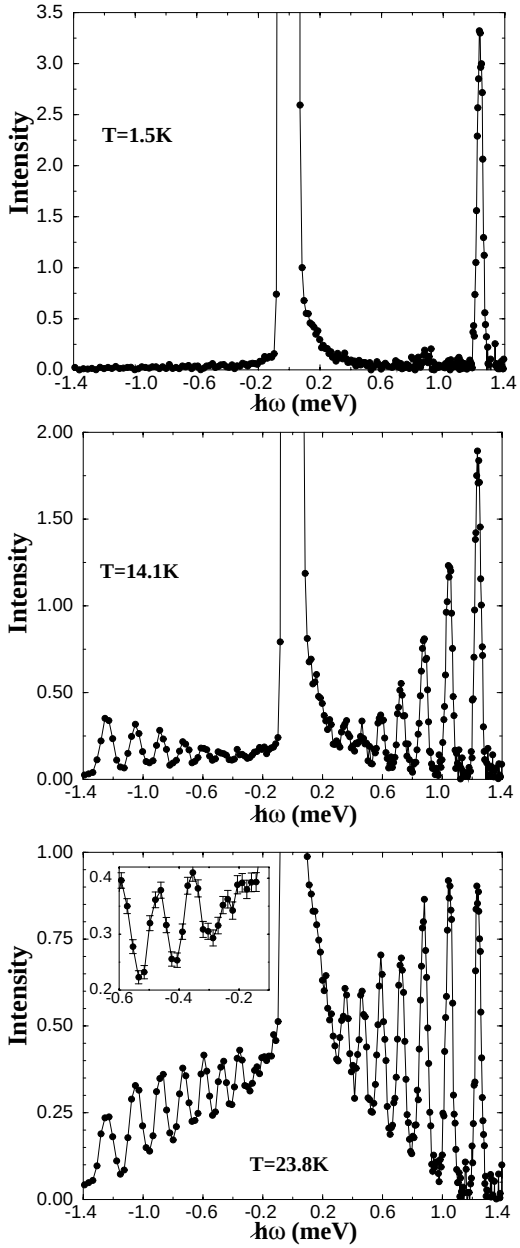

FIG. 1. Energy spectra at three temperatures (raw data). The intensity units are the same but the scales are different for all spectra. In the inset, the low-energy range on the sample energy loss side.

In the approximation of a $S = 10$ single spin Hamiltonian, the magnetic intensity is written as [18]

$$S(\mathbf{Q}, \hbar\omega) = N(\gamma_N r_e/2)^2 g^2 f^2(\mathbf{Q}) \times \sum_{i,f} p_i |\langle f|S_\perp|i\rangle|^2 \delta(\hbar\omega - (E_f - E_i)),$$

with

$$|\langle f|S_\perp|i\rangle|^2 = 1/3(2|\langle f|S_z|i\rangle|^2 + |\langle f|S_+|i\rangle|^2 + |\langle f|S_-|i\rangle|^2). \quad (1)$$

$S_\perp$ is the spin component perpendicular to the scattering vector $\mathbf{Q}$. $p_i = \exp(-E_i/k_BT)/\sum_i \exp(-E_i/k_BT)$ is the Boltzmann factor of the level i. The delta function is convoluted by the experimental resolution function. The eigenstates $|i\rangle$ have the energies E_i obtained by a diagonalization of the spin Hamiltonian. We adopt the spin Hamiltonian used to interpret EPR [9], magnetization [19], and far-IR experiments [11],

$$H = D[S_z^2 - 1/3S(S+1)] + B_4^0 O_4^0 + B_4^4 O_4^4, \quad (2)$$

with $O_4^0 = 35S_z^4 - [30S(S+1) - 25]S_z^2 - 6S(S+1) + 3S^2(S+1)^2$ and $O_4^4 = 1/2(S_+^4 + S_-^4)$.

From Eq. (1), it follows that only the transitions with $\Delta M = 0$ or ± 1 are allowed. When only the diagonal terms are considered in Eq. (2) ($B_4^4 = 0$), the $S = 10$ manifold splits into 11 sublevels corresponding to $M = \pm 10, 9, \ldots, 0$. The $\pm M$ degeneracy is not lifted, and when all possible levels are populated we expect to observe nine $\Delta M \pm 1$ transitions on either side of the spectrum. Seven of these correspond to the well-resolved peaks observed at 15 and 23.8 K in Fig. 1. The decreasing energy spacing with decreasing energy transfer arises mainly from the fourth-order B_4^0 term.

As a first step in our quantitative data analysis, in terms of Eqs. (1) and (2), we neglected the transverse term B_4^4 which is known to be small. The positions and relative intensities of the five most intense excitations are well reproduced, and the fitted values of the parameters [$D = -0.457(2)$ cm^{-1}, $B_4^0 = -2.33(4) \times 10^{-5}$ cm^{-1}] agree with the determination of Barra *et al.* by EPR [9] and Mukhin *et al.* by far-IR spectroscopy [11]. However, this simplified model overestimates the intensities of the excitations below 0.3 meV, which involve energy levels close to the top of the anisotropy barrier.

In a second step, we therefore took the off-diagonal term B_4^4 into account. A nonzero B_4^4 induces a mixing of energy levels with different M that becomes more and more effective on approaching the top of the barrier. This is illustrated in Fig. 2, where the positions of the energy levels E_i are plotted versus B_4^4, for given B_4^0 and D. The energies of the highest excited states strongly depend on B_4^4, and the degeneracy of the $M = \pm 2$ and ± 4 levels is lifted for nonzero B_4^4. At the top of Fig. 3, we show the calculated intensities at 23.8 K for three different B_4^4 values, using the experimental energy resolution, in the energy transfer range $(-0.5, 0.5)$ meV. In this range the position, shape, and intensities of the inelastic peaks strongly depend on B_4^4, whereas the other peaks remain unaffected. Depending on the B_4^4 value (3 or 4 $\times 10^{-5}$ cm^{-1}), the energy transfer at 0.2 meV corresponds either to a minimum or to a maximum intensity, respectively. Therefore, only B_4^4 values in a very narrow range can explain the experimental behavior. We find that $B_4^4 = \pm 3.0(5) \times 10^{-5}$ cm^{-1} gives the best agreement with the data. This value is slightly lower and more accurate than the one reported by Barra *et al.* [$B_4^4 = \pm 4(1) \times 10^{-5}$ cm^{-1}]. The sign of B_4^4 is undetermined, owing to the symmetry of the Hamiltonian. In Fig. 3, we present the results of the model calculation with the best fitted values $D = -0.457$ cm^{-1}, $B_4^0 = -2.33 \times 10^{-5}$ cm^{-1}, and $B_4^4 = \pm 3.0(5) \times 10^{-5}$ cm^{-1}.

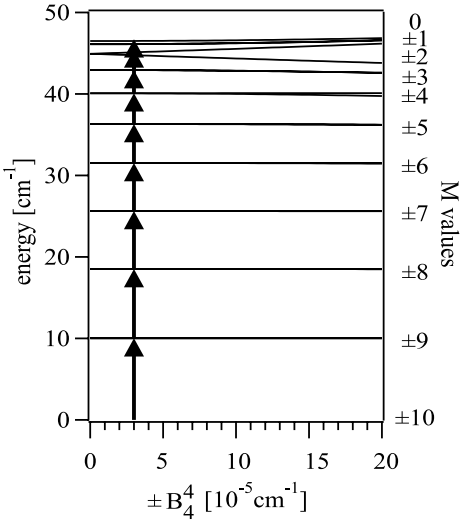

FIG. 2. Energy sublevels of the $S = 10$ ground state versus B_4^4, as calculated for $D = -0.457$ cm^{-1}, $B_4^0 = -2.33 \times 10^{-5}$ cm^{-1}.

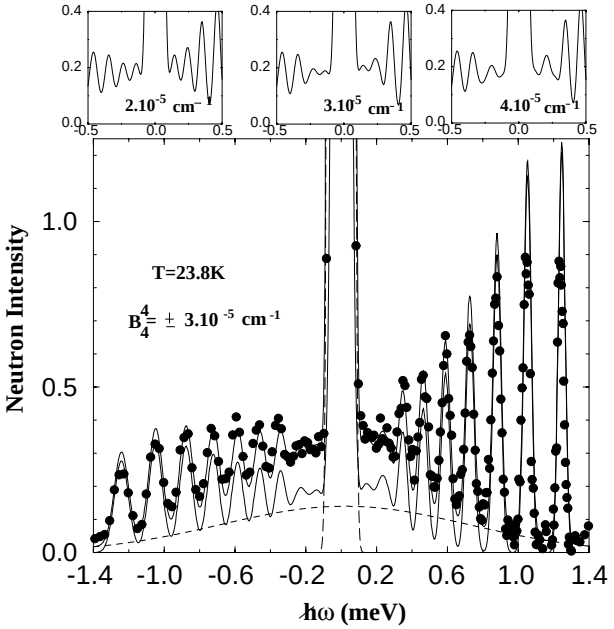

FIG. 3. Energy spectra: filled circles are data corrected for the Gaussian signal observed at 1.5 K near zero energy transfer. The intensity calculation (thin line), Lorentzian background (dashed line), elastic intensity (long-dashed line), and the sum of all components (thick line) are also plotted. At the top of the figure, intensity calculations for three B_4^4 values are shown.

To compare with experimental data at 23.8 K, we added a Lorentzian quasielastic background, probably due to hydrogen. The agreement with experiment is excellent. The small reduction of the observed intensities near 1.2 meV is ascribed to a partial population of higher-energy cluster spin states. The single spin $S = 10$ model breaks down above 30 K [11].

The main result coming out of our analysis is the precise determination in zero field of the coefficient B_4^4 in the transverse term. The presence of nondiagonal terms in the spin Hamiltonian has been searched for by many theoreticians and experimentalists, since only components which do not commute with S_z could induce tunneling. In zero field, a term $C(S_+^4 + S_-^4)$ is the lowest-order spin Hamiltonian allowed by tetragonal symmetry. Such a term allows tunneling with $\Delta M = \pm 4$, as observed experimentally in the magnetization. In a recent model calculation [20], the relaxation data by Thomas *et al.* [4] were better reproduced by our new B_4^4 value than the old one in literature, allowing a better quantitative understanding of the dominant tunneling process. However, other transverse terms are required to explain the tunneling transitions with $\Delta M = \pm 1$. Politi *et al.* [5] have also argued that if only this fourth-order transverse term was involved, a very small field such as the earth field would destroy tunneling. Other transverse terms deriving from dipolar coupling [21], hyperfine interactions [19,21] or a spin-phonon coupling mechanism [5] have been suggested in addition to the previous one. Up to now, they have not been certified, and our results provide no evidence for their existence.

The analysis presented above is based on the assumption of a "single spin" ground state. This simple model describes the low-energy excitations presented in this work very well. However, our earlier INS experiments at higher energies [14] show that excitations involving other spin states are rather close to the $S = 10$ ground state. Recent measurements by magnetization [19] or heat capacity [22] also point out the influence of excited states with different S values. Several microscopic descriptions of the $S = 10$ ground state have been proposed [2,9,23], which involve different coupling schemes between the individual spins. Because of the large number of cluster spin states, 10^8 in the general case, simplifications must be made by considering the hierarchy of interactions between individual spins. Very recently, a new formalism for the energy was proposed [24]. Following the Florentine coupling scheme [2], Mn_{12}-ac is described by four dimers Mn^{3+}-Mn^{4+} with spin $s = 1/2$, and four Mn^{3+} ions ($S = 2$), coupled by isotropic exchange interactions. The dominant exchange coupling is between the spins inside a dimer, as first suggested by [2], and in agreement with recent magnetic measurements in the megagauss range [25]. The Hamiltonian includes relativistic anisotropic interactions, the Dzyaloshinskii-Moriya ones being the most important. This model qualitatively explains the spin excitations previously measured by INS up to 12 meV [14]. We believe that our new experimental results will be a crucial checkpoint for further theoretical work.

[1] T. Lis, Acta Crystallogr. Sect. B **36**, 2042 (1980).
[2] R. Sessoli, D. Gatteschi, A. Caneschi, and M. A. Novak, Nature (London) **365**, 141 (1993); R. Sessoli *et al.*, J. Am. Chem. Soc. **15**, 1804 (1993).
[3] J. M. Hernandez, X. X. Zhang, F. Luis, J. Bartolomé, J. Tejada, and R. Ziolo, Europhys. Lett. **35**, 301 (1996).
[4] L. Thomas, F. Lionti, R. Ballou, D. Gatteschi, R. Sessoli, and B. Barbara, Nature (London) **383**, 145 (1996); J. R. Friedman, M. P. Sarachik, J. Tejada, and R. Ziolo, Phys. Rev. Lett. **76**, 3830 (1996).
[5] P. Politi, A. Rettori, F. Hartmann-Boutron, and J. Villain, Phys. Rev. Lett. **75**, 537 (1995); A. Fort, A. Rettori, J. Villain, D. Gatteschi, and R. Sessoli, Phys. Rev. Lett. **80**, 612 (1998).
[6] D. A. Garanin and E. M. Chudnovsky, Phys. Rev. B **56**, 11 102 (1997).
[7] L. Gunther, Europhys. Lett. B **39**, 1 (1997).
[8] M. R. Pederson and S. N. Khanna, Phys. Rev. B **59**, R693 (1999).
[9] A. L. Barra, D. Gatteschi, and R. Sessoli, Phys. Rev. B **56**, 8192 (1997).
[10] S. Hill, J. Perenboom, N. S. Dalal, T. Hathaway, T. Stalcup, and J. S. Brooks, Phys. Rev. Lett. **80**, 2453 (1998).
[11] A. A. Mukhin, V. D. Travkin, A. K. Zvezdin, S. P. Lebedev, A. Caneschi, and D. Gatteschi, Europhys. Lett. **44**, 778 (1998).
[12] H. U. Güdel in *Molecular Magnetism*, edited by E. Coronado *et al.*, NATO ASI, Ser. E, Vol. 321 (Kluwer, Amsterdam, 1996), pp. 229–242.
[13] R. Caciuffo, G. Amoretti, A. Murani, R. Sessoli, A. Caneschi, and D. Gatteschi, Phys. Rev. Lett. **81**, 4744 (1998).
[14] M. Hennion, L. Pardi, I. Mirebeau, E. Suard, R. Sessoli, and A. Caneschi, Phys. Rev. B **56**, 8819 (1997).
[15] J. Rodriguez-Carvajal, Physica (Amsterdam) **192B**, 55 (1993).
[16] Z. Sun *et al.*, Inorg. Chem. **37**, 4758 (1998).
[17] W. Wernsdorfer, R. Sessoli, and D. Gatteschi, cond-mat/990450.
[18] R. J. Birgenau, J. Phys. Chem. Solids **33**, 59 (1972).
[19] B. Barbara, L. Thomas, F. Lionti, A. Sulpice, and A. Caneschi, J. Magn. Magn. Mater. **177–181**, 1324 (1998).
[20] D. Loss (private communication).
[21] F. Luis, J. Bartolomé, J. F. Fernandez, J. Tejada, J. M. Hernandez, X. X. Zhang, and R. Ziolo, Phys. Rev. B **55**, 11 448 (1997).
[22] A. M. Gomes, M. A. Novak, R. Sessoli, A. Caneschi, and D. Gatteschi, Phys. Rev. B **57**, 5021 (1998); F. Fominaya, J. Villain, P. Gandit, J. Chaussy, and A. Caneschi, Phys. Rev. Lett. **79**, 1126 (1998).
[23] A. K. Zvezdin and A. Popov, JETP **82**, 1140 (1996).
[24] M. I. Katsnelson, V. V. Dobrovitski, and B. N. Harmon, Phys. Rev. B **59**, 6919 (1999).
[25] A. A. Mukhin *et al.* (unpublished).